Critical current densities and the structural quality of 3- and 4-μm-thick superconducting $YBa_2Cu_3O_7$ layers synthesized using the *ex situ* process

Vyacheslav F. Solovyov,[a] Harold J. Wiesmann, and Masaki Suenaga
Condensed Matter Physics and Materials Science Department, Brookhaven National Laboratory, 76 Cornell Avenue, Upton, New York 11973, USA

(Received 6 March 2007; accepted 9 July 2007; published online 5 September 2007)

In this work, we used quantitative x-ray diffraction measurements and optical metallography to investigate the relationship between structural quality and critical current densities J_c for 3- and 4-μm-thick $YBa_2Cu_3O_7$ (YBCO) films grown on CeO_2-buffered Ni–W substrates by the BaF_2 process. The J_c of the films was shown to be approximately: (1) proportional to the intensity of the YBCO (006) diffraction line, and (2) inversely proportional to the average grain size of the *c*-axis oriented YBCO as determined from optical micrographs of polished surface of the films. We conclude that to achieve J_cs well above 10^6 A/cm^2 in self-field and at 77 K, it is critical to suppress the formation of randomly oriented YBCO grains while maintaining high crystallographic quality of the *c*-axis oriented part of the film. The quality of the *c*-axis oriented YBCO was found to be strongly dependent on the YBCO grains size—e.g., the grains, which are smaller than 10 μm, are required for high J_c films. The fine-grain high J_c films can be synthesized under processing conditions that promote a high rate of nucleation of *c*-axis oriented YBCO. © *2007 American Institute of Physics*. [DOI: 10.1063/1.2773997]

I. INTRODUCTION

Creating a practical superconductor often requires finding a fine balance between introducing sufficient amounts of small microstructural defects and achieving a high crystallographic order for a given superconducting material. Small-scale defects, when they are present in large numbers, can effectively pin magnetic flux, thus enabling high critical currents in external magnetic fields. Obviously, defects cannot be added indiscriminately, since they also reduce the effective cross section of the conductor and degrade structural quality of the superconducting matrix, eventually negating the benefits of enhanced pinning. The structural perfection, which determines critical temperatures T_c, of a superconductor, is especially important for $YBa_2Cu_3O_7$ (YBCO) coated conductors, which are now manufactured for power applications at or near the liquid nitrogen temperature, 77 K. Because the difference between T_c(~92.5 K) of YBCO and the operating temperature, ~77 K, is only 16% of T_c (for comparison, it is ~50% for a NbTi wire operating at 4.2 K), even a minor reduction in T_c has negative consequences for the reliability of electrical equipment based on YBCO conductors. Additionally, due to its exceptionally small superconducting coherence length, even minor structural imperfections, such as grain boundaries, can block the supercurrent in the YBCO layer. These factors emphasize the need to make the YBCO layer, in a high-performance coated conductor, nearly perfect in structure and thus "transparent" for the supercurrent.

It has been demonstrated that thin (<1 μm) YBCO layers with an excellent *c*-axis texture and extremely high J_c can be grown by a variety of deposition methods.[1] However, economic considerations dictate that the YBCO layer in a practical coated conductor has to have a thickness of over ~3 μm and a J_c (self-field at 77 K) >1 MA/cm^2 to carry critical currents high enough for power applications. Unfortunately, simply adding an extra thickness of YBCO did not work for almost all popular deposition techniques. For example, it was found that the overall critical current of the films, deposited by pulse laser deposition (PLD), almost stopped increasing when the film thickness surpassed the ~1 μm threshold, i.e., the additional YBCO deposited on the 1-μm-thick film carried very little supercurrent.[2] Recent advances in PLD technology and the synthesis of effective pinning centers allowed several groups to break the 1-μm thickness barrier and demonstrate impressive J_c values for multi-micrometer-thick YBCO films on metal substrates.[3–5]

These results are very important as a proof of principle and demonstrate the potential of YBCO material. The BaF_2-based *ex situ* process is considered to be a scalable route for the production of thick YBCO coatings. One variation of this process, called metal-organic decomposition (MOD), is now being employed by the American Superconductor Corporation for the large-scale production of coated YBCO conductors.[6] In this work, we use another variation of the *ex situ* process, where a vacuum deposition method is used to prepare the precursor films.[7,8] (For simplicity, in the following we call this the BaF_2 process.) This method allows the deposition of crack-free dense multi-micrometer-thick YBCO precursor films that are well suited for the study of the *ex situ* conversion process. In our previous work, we outlined a successful strategy for achieving self-field J_c in excess of 1 MA/cm^2 in 3- and 4-μm-thick YBCO layers on buffered metallic tapes. In essence, we optimized the pro-

[a]Electronic mail: solov@bnl.gov

 © 2007 American Institute of Physics

Downloaded 12 Sep 2007 to 130.199.3.130. Redistribution subject to AIP license or copyright, see http://jap.aip.org/jap/copyright.jsp

cessing conditions to promote the nucleation of high-density *c*-axis oriented YBCO, while limiting the nucleation of randomly oriented YBCO grains.[9] In the present work, we focused on the examination of the structural properties—as determined by x-ray diffraction and optical microscopy—of a statistically meaningful set of 3- and 4-μm-thick YBCO films that were processed under the growth conditions described in Ref. 9. The results are used to develop a systematic relationship between the structural quality and the transport critical current densities J_c of thick YBCO films by the BaF_2 process.

II. EXPERIMENT

The metallic substrates, provided by the American Superconductor Corporation, were textured Ni–W alloy tapes (RABiTS™)[10] coated with epitaxial oxide buffer layers. The substrate was comprised of the following layers in sequence from the alloy tape to the top oxide buffer: 75 μm (Ni-5 at. %W)−75 nm Y_2O_3−75 nm (*Y* stabilized ZrO_2) −75 nm CeO_2. The substrates had an average in-plane texture of 6.9° and an out-of-plane texture of 5.0°. The fluorinated precursor films, Y-BaF_2-Cu, were deposited on the substrates using vacuum coevaporation of Cu, Y, and BaF_2 at ambient temperature. Fluxes of these elements and the molecule were independently controlled to yield an elemental composition to $Y_{1.4}Ba_2Cu_3$ for the films at a combined deposition rate of 10 nm/s. We routinely achieved the composition within 5% of the target as confirmed by inductively coupled plasma (ICP) analyses using a JY-Horiba ULTIMA-2 ICP spectrometer. During the deposition, we additionally provided a flux of water vapor directed at the substrate by a specially designed showerhead. The purpose of adding water was to partially oxidize the yttrium in the precursor films. Otherwise, shortly after removing the precursor films from the deposition chamber, the films would react uncontrollably with atmospheric moisture and often delaminate from the substrate. Directed injection of water vapor at the substrate area allowed us to stabilize the yttrium oxidation state and, at the same time, keep the pressure in the deposition chamber below 10^{-5} Torr, which helped to avoid arcing of the electron-beam guns. When removed from the deposition chamber, the films were black, shiny, and, most importantly, chemically stable in the laboratory environment. After the deposition of the precursor films and prior to the conversion of the films to YBCO, the samples were annealed for 1 h at 400 °C in a gas atmosphere of 70 Torr of water vapor and 100 mTorr of oxygen, with the balance being nitrogen gas. This prereaction annealing was introduced for the oxidation of copper to copper oxide and the conversion of yttrium and barium to a textured oxyfluoride.[11–13] We added this step after realizing that the thick precursor films did not have sufficient time to oxidize and texture the transient phases thoroughly before the films reached the conversion temperature. Without this pretreatment, the rates of nucleation of epitaxial *c*-axis oriented YBCO were very low. Finally, the precursor films were converted to YBCO in a process-gas mixture at subatmospheric pressures.[14] The processing conditions used in this study were as follows: the overall process-gas and water vapor pressures were kept constant at 20 and 0.5 Torr, respectively, and the temperature was 735 °C. The oxygen partial pressures (40–300 mT) and the growth rates (0.2 and 0.7 nm/s) were the only parameters that were varied for this study. These processing conditions were same as those described in Ref. 9. As was previously done, the slower growth rate was achieved by surrounding the sample by a quartz baffle, which restricted the flow of HF gas from the sample surface.

The primary goal of this work was to relate the average structural properties of 3- and 4-μm-thick YBCO films by the BaF_2 process to their critical-current densities. For this purpose, we used $\theta-2\theta$ x-ray-diffraction measurements of the as-processed YBCO films and optical microscopy of the mechanically polished YBCO films. We selected the peak intensities of two reflections in the $\theta-2\theta$ x-ray-diffraction spectra of the YBCO films as the signatures of the average structural quality of the films. These were (103, 013) [further YBCO (103)] at $2\theta=32.8°$ and (006) at $2\theta=46°$ reflections. The YBCO (103) line was used to quantify the contents of randomly oriented grains in the films since it is the strongest line in the diffraction spectrum of powder YBCO.[15] (Interestingly *a*-axis oriented YBCO grains were hardly found in these films.) The other line, YBCO (006), is the strongest (00*l*) reflection and thus was chosen as an indicator of the amount and the structural quality of the *c*-axis oriented part of the films. In order to rule out the influence of line broadening on the peak intensities of the YBCO (006) line due to any *c*-axis misalignment, line broadening of the YBCO (006) was measured on a four-circle goniometer for five samples with widely different YBCO (006) line intensities. For all samples, the out-of-plane and in-plane misalignments of the YBCO layer were the same with those of the Ni–W substrate, and both were ~6° for the full width half maximum.[6] It is well known that the absolute intensities of (00*l*) lines from YBCO films have to be used with caution, since these intensities are strongly affected by the sample misalignment with respect to the x-ray beam and the detector of a diffractometer. This is particularly relevant for YBCO coated tapes that are never ideally flat; the tapes tend to bend slightly from the differential thermal contractions of the materials in the tape during the cooldown from reaction temperatures. To minimize this factor, the YBCO (006) intensity was divided by that of Ni–W (002) line at $2\theta=52°$. We assumed that both of the YBCO and Ni–W peaks would change proportionally in response to the small tilt and/or the warping of the tape coupons, and thus the YBCO (006)/Ni–W (002) ratio was used as a reliable gauge of the structural quality. This ratio, however, is device specific and can only be used to compare spectra recorded on the same diffractometer.

To reveal microstructural morphologies within the thick films, it was sufficient to remove an upper layer (~1 μm) of the YBCO films by metallurgical planar polishing. The polished surface was then inspected under polarized light and the Nomarski (differential interference contrast) mode of a Riechert–Jung MEF3 microscope. By adjusting the shift of the Nomarski prism, we were able to obtain clear images of

Downloaded 12 Sep 2007 to 130.199.3.130. Redistribution subject to AIP license or copyright, see http://jap.aip.org/jap/copyright.jsp

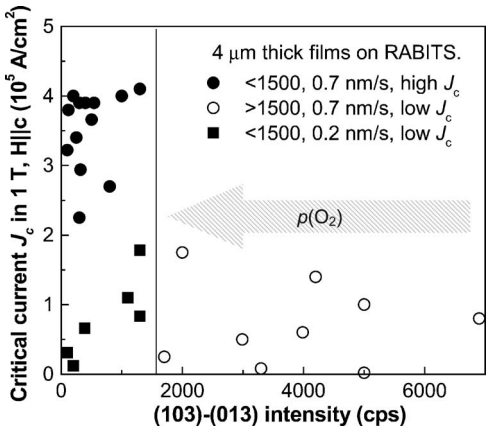

FIG. 1. Critical current density $J_c(H\|c)$ of 4 μm thick films at 1 T and 77 K vs the intensity of (103)(013) YBCO reflection, corresponding to the contents of the randomly oriented YBCO, is shown. Circles and squares denote samples grown at the rates of 0.7 and 0.2 nm/s, respectively. Open circles denote the samples with the intensity over the "threshold" value of 1500 cps. (The solid vertical line indicates the threshold value.) In these samples, J_c is severely reduced by the randomly oriented YBCO grains.

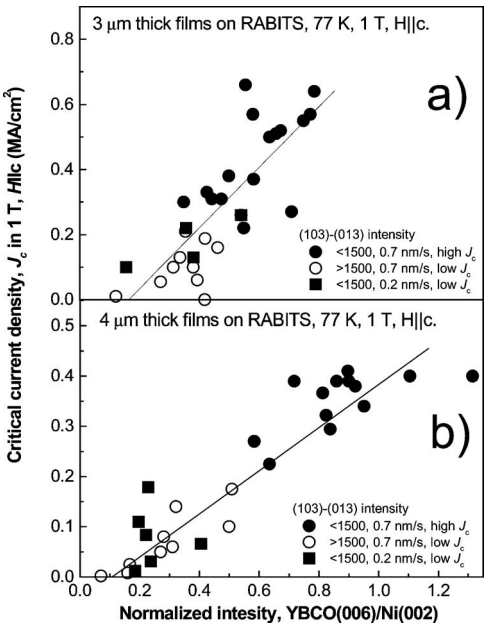

FIG. 2. Critical current density at 1 T $J_c(H\|c)$ and 77 K vs the normalized intensity (006)YBCO/(002)Ni for (a) 3- and (b) 4-μm-thick YBCO films on RABITS™ tapes are shown. The same specimen-identification symbols are used as those in Fig. 1.

the YBCO grains. Standard software for image analysis was used to calculate the average grain size from the areas containing over 100 YBCO grains.

Critical currents I_c were measured by a dc four-point transport method in liquid nitrogen (77 K) using an electric-field criterion of 0.1 μV/mm. Typical critical currents of 4-μm-thick samples (3×10 mm^2) were too large to be directly measured at self-field. Therefore, the I_cs of these films were measured in an external magnetic field of 1 T applied perpendicularly to the film plane ($H\|c$). For 3-μm-thick films, we reduced the sample width to a 0.6 mm wide bridge so that the I_c could be measured both at self-field and 1 T, $H\|c$, for the entire set of 30 3-μm-thick films.

III. RESULTS AND DISCUSSION

A. Structure versus J_c

It is well known that presence of non-c-axis oriented YBCO has a strong negative effect on the J_c of epitaxial YBCO layers. Therefore, we correlated the J_c values of 30 4-μm-thick YBCO films and the content of the randomly oriented grains by plotting their critical current densities $J_c(1\ \mathrm{T})$ at $\mu_0 H=1$ T against the peak intensities of the (103) line in Fig. 1. It followed from Fig. 1 that $J_c(1\ \mathrm{T})$ did not correlate with the intensity of the (103) line until the intensity surpassed an approximate threshold value of 1500 counts beyond which the J_c of the films dropped substantially.

In Fig. 1, the data points corresponding to the samples processed at the growth rate of ~0.7 nm/s are presented as circles. Among these, those with the (103) intensities over the threshold are shown as open circles and those below are in solid circles. Also, those films that are made with a growth rate of ~0.2 nm/s are indicated by solid squares. These differences in the properties of the films for a given growth rate are due to the variations of oxygen partial pressure $p(O_2)$ in the processing atmosphere during YBCO growth. In this set, the samples were processed at $p(O_2)$ values ranging from 40–300 mTorr, which resulted in either predominantly randomly oriented YBCO grains at high $p(O_2)>200$ mTorr, or c-axis oriented YBCO layers at low $p(O_2)<100$ mTorr. This effect of $p(O_2)$ variations on the structure and J_c is schematically indicated by a dashed arrow in the Fig. 1.

The randomly oriented YBCO platelets appeared at the sample surface as 40 μm long 4 μm wide rods, and could be easily detected by optical microscopy. Such observations established an approximate linear relationship between the (103) intensity and the areal density of randomly oriented YBCO grains. The threshold intensity, mentioned above, approximately corresponded to a situation when the randomly oriented grains began to overlap thus severely reducing pathway for the supercurrent and lowering J_c.

We conclude from Fig. 1 that the content of randomly oriented grains, inferred form the x-ray-diffraction spectra, offers limited information on the structural quality of the films and cannot be directly related to the J_c values. Excessive content of random orientation does not account for significant variations in J_c of a large set of 0.7 nm/s samples (closed circles in Fig. 1) and all the samples processed at 0.2 nm/s (represented by solid squares in Fig. 1). In these cases, the (103) intensity is quite low yet the values of their J_c can also be low indicating the presence of factor(s), other than non-c-axis oriented platelets, that contribute to the J_c variation.

Searching for a better structural parameter to represent the variations in J_c of these films, we plotted the J_c data set for the 3- and 4-μm-thick films using the ratio of YBCO(006) and Ni-W(002) lines for the abscissa as shown in Figs. 2(a) and 2(b). For the 3- and 4-μm-thick films, J_c at 1 T are plotted in Figs. 2(a) and 2(b). For these sets of the thick films, we retained the data point labeling system used in Fig. 1. Best-fit approximations, shown as solid lines, dem-

Downloaded 12 Sep 2007 to 130.199.3.130. Redistribution subject to AIP license or copyright, see http://jap.aip.org/jap/copyright.jsp

onstrate the approximately linear relationship between J_c and the YBCO(006)/Ni-W(002) intensity ratio for both 3- and 4-μm thick films. Such a universality of J_c response to the intensity ratio may seem surprising; however, it should be mentioned that the intensity of the (006) line is a compound structural characteristic, depending on both the abundance and the degree of the crystallographic order of the *c*-axis-oriented YBCO material. Thus, a sample with low intensities of both (103) and (006) lines most likely contains significant crystallographic disorder, which results in a suppression the structural factors for (00*l*) reflections and associated drop in J_c. Notably, all the samples processed at a growth rate of 0.2 nm/s fall into this category: they are practically void of randomly oriented grains but have weak (00*l*) line intensities and low J_c. On the other hand, for the samples with a lot of randomly oriented grains i.e., the (103) intensities $> \sim 1500$ counts (open circles), the most probable cause for the reduced (006) line intensity ratio is the displacement of the *c*-axis oriented with the randomly oriented one.

B. Grain size, critical current density, and structural quality

The above linear relationship between J_c and the (006) intensity ratio indicated that structural factors played a major role in performance of thick YBCO films. However, x-ray diffraction measurements provided only average structural information, therefore we needed to complement the x-ray data with some other measurements which provide the local structural information. In a search for the "hidden" factor, the surfaces of the films were initially screened by optical and scanning electron microscopy. These observations provided little clues on the disorder since the surface was rather featureless, except for the samples with very low J_c, which showed signs of granularity or high densities of randomly oriented YBCO as described previously.[9] In contrast, when the approximately 1-μm-thick top layer of a YBCO film was removed by mechanical polishing, the grains of YBCO could be easily observed by optical microscopy in the Nomarski mode. After these experiments, it became obvious that the samples with high J_c were comprised of the *c*-axis oriented YBCO grains much smaller than those with low J_c. Figures 3(a) and 3(b) are examples of optical Nomarski-contrast micrographs of two polished 3-μm-thick YBCO films, illustrating the differences in the grain sizes between these samples. The values of J_c for the films in Figs. 3(a) and 3(b) were 0.3 and 1.4×10^6 A/cm^2 at self-field, respectively. Thus, it was realized that the size of the *c*-axis-oriented YBCO grains was the signature for the hidden microstructural factor responsible for the J_c variations in the samples with low (103) intensities, indicated by closed symbols in Fig. 2.

X-ray-diffraction measurements of these samples, shown in Fig. 3 proved that these were completely *c*-axis oriented YBCO films; but as noted above, their J_cs were very different due to the differences in the grain size. The grains in Fig. 3(a) were very coarse with an average grain size of ~ 17 μm in diameter; while those in Fig. 3(b) were fine grain and one-half as large as those in Fig. 3(a), ~ 8 μm. Using the micrographs similar to ones shown in Fig. 3, we were able to

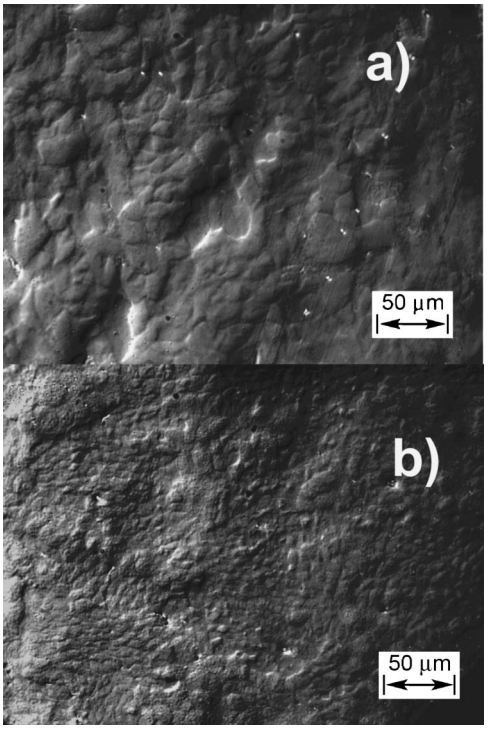

FIG. 3. Nomarsky optical contrast of two polished 3-μm-thick films with different grain sizes. Panel (a) shows a sample with large 17 ± 4 μm grains and J_c (self-field)=0.3 MA/cm^2. Panel (b) shows a sample with smaller, 8 ± 1 μm, grains and J_c (self-field)=1.4 MA/cm^2.

correlate the grain size to the critical current density. This is presented in Fig. 4 for a set of nine 3-μm-thick films by plotting the self-field J_c versus inverse grain size, $1/d$. The solid line in Fig. 4 indicates that an approximate dependence of J_c on $1/d$ and $J_c \propto 1/d - 1/d_c$ with $d_c=47$ μm provided the best fit to the data. Figure 4 shows that YBCO grain coarsening leads to a drastic decrease in their J_c, and that a sample with the grains larger than ~ 50 μm would have virtually zero J_c. The optical contrast technique could not resolve grains smaller than 7 μm; these samples looked featureless. Extrapolating the $1/d$ approximation in Fig. 4, we estimate that samples with $J_c \sim 2\times10^6$ A/cm^2 had an average grain size of 5–6 μm. Figures 2 and 4 represent the principal result of this study, which indicates a direction for

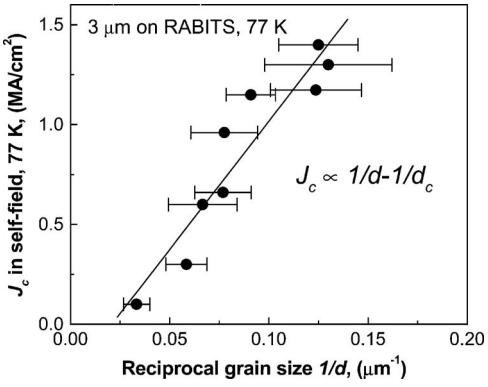

FIG. 4. Critical current density at self-field and 77 K is plotted as a function of the inverse grain size of 3-μm-thick YBCO films. The grain size was determined from analysis of optical micrographs similar to those shown in Fig. 3.

Downloaded 12 Sep 2007 to 130.199.3.130. Redistribution subject to AIP license or copyright, see http://jap.aip.org/jap/copyright.jsp

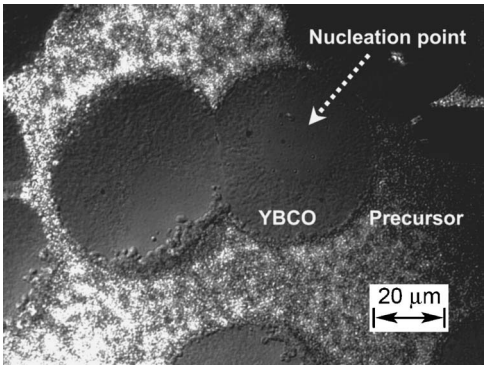

FIG. 5. An optical image of a partially converted YBCO film showing large circular *c*-axis oriented YBCO grains surrounded by the unreacted precursor material. Note the appearance of YBCO nuclei changes from solid at the central to porous at the outer region.

improving the performance of thick YBCO layers by improving the structure, as measured by the (006) intensity, achieved by the refinement of the YBCO grains.

In order to clarify the structural change brought about by the grain coarsening, we examined isolated *c*-axis oriented YBCO nuclei, which were specially grown to be very large but not totally merged with the adjacent nuclei. This was accomplished by partially processing a 3-μm-thick film under very low $p(O_2)$. Under these processing conditions, we obtained very sparse YBCO nuclei ($\sim$50 μm apart), which were allowed to ripen up to $\sim$40 μm in diameter. After that, the sample was quenched to avoid the impingement of the grains. According to Fig. 4, if this film were fully processed, it would have grains of 50 μm in diameter and almost zero J_c. To observe the nuclei, $\sim$2-μm-thick upper portion of the film, which was mostly unreacted precursor, was removed by planar polishing, and the polished surface was examined under an optical microscope in a polarized light mode. Under this observation condition, the YBCO nuclei appeared as dark disks and unreacted precursor appeared as the light colored background shown in Fig. 5. Generally, the centers of the nuclei were the approximate locations of the nucleation sites.

Upon observing these nuclei, we noted that a typical nucleus over $\sim$20 μm in diameter had two clearly distinguishable parts: a dense inner core, approximately 20 μm in diameter, and an outer region with porous appearance. This two-part structure can be easily seen in Fig. 5 in both nuclei. Evidently, the nucleus ripening is a complex process and the structural quality of the YBCO material appears to degrade significantly as the nuclei expand in a lateral (parallel to the basal plane) direction beyond their diameters of $\sim$20 μm. Furthermore, since similar disordered structures are observed in films with large YBCO grains after the films were completely reacted, the outer areas of the large grains are structurally disordered and likely contribute to the reduction of the (006) intensity ratio of the coarse-grained films. This in turn degrades the current carrying capacity of the whole YBCO layer. On the other hand, when the nuclei are close to each other, i.e., high nuclei densities, the lateral growth of the grains becomes limited by the impingement of the neighboring nuclei, and the growth of the YBCO grains in the *c*-axis direction becomes the dominant mode for the precursor-YBCO reaction. Thus, the growth of the fine-grained high J_c YBCO layers proceeds primarily in the *c*-axis direction (normal to the substrate), while a coarse-grained low-J_c YBCO layer is a product of the growth mode dominated by the basal plane (parallel to the substrate) growth. We conclude that the disorder accumulation during excessive lateral expansion of the nuclei is a plausible explanation for J_c degradation in coarse-grained films. Even though the samples with grains smaller than 20 μm in diameter appear dense and uniform, according to Fig. 4, we gain J_c by reducing the grain size below 20 μm. This possibly means that the lateral growth still has damaging effect on the structure in this grain size range, but the damage is not detectable by optical microscopy.

Our work demonstrates that J_c can be significantly improved by reducing the grain size below 10 μm; however, how far the $J_c \sim 1/d$ dependence extends in the low d region is still an open question. One limitation may be the grain boundary (GB) permeability. The GB permeability becomes a critical factor for YBCO layers deposited on industrial RABiTS™ substrates, which are comprised of biaxially aligned large ($\approx$50 μm) Ni–W grains with associated low-angle GBs. The YBCO layer, epitaxially grown on such a substrate, would typically consist of smaller ($\ll$10 μm for high J_c samples) YBCO grains, which inherit the orientation of the Ni–W substrate and form a new GB network. It has been demonstrated[16] that pronounced lateral growth, encountered in *ex situ* films, causes the YBCO GB to meander, i.e., significantly (on several micron-scale) deviate from GB of the substrate. Meandering GBs turned out to be much more tolerant of the grain misorientation, and impressively high J_cs have been demonstrated for the misorientation angles as high as 10°.[16] In contrast, films prepared by PLD had very high nuclei density, virtually no lateral growth, and straight grain boundaries. Straight grain boundaries in PLD films deposited on RABiTS™ substrates exhibited a typical[17] rapid decline in the J_c with the misorientation angle, resulting in a lower overall I_c of the PLD YBCO layer compared with the *ex situ* grown YBCO. By reducing the grain size of the *ex situ* grown YBCO, we suppress the lateral growth and thus improve the structure. However, at the same time, we reduce the GB meandering (make the GB straighter), which may have negative effects for the GB permeability and eventually reduce the overall J_c when d becomes too low.

Microscopic details of the disorder, which was produced by extensive lateral growth of the nuclei, remain unclear. Isolated YBCO nuclei similar to those shown in Fig. 5 were studied by Raman microscopy for signs of cation substitution. Scans of the entire area of a nucleus, 40-μm in diameter, did not detect significant changes in the Raman spectrum across the nucleus.[18] At this point, the exact nature of the disorder in the large grains is undetermined. Further studies are needed to clarify this issue, perhaps by employing transmission electron microscopy techniques.

IV. SUMMARY

In summary, we have identified two principal directions for achieving high critical currents in thick YBCO films by

Downloaded 12 Sep 2007 to 130.199.3.130. Redistribution subject to AIP license or copyright, see http://jap.aip.org/jap/copyright.jsp

the BaF_2 process: (1) minimization of the volumetric displacement of the *c*-axis oriented YBCO by the randomly oriented grains and (2) improvement in the crystallographic order of *c*-axis oriented YBCO grains by a reduction in the grain size. This is realized by setting processing conditions in such a way that yields a high density of *c*-axis oriented nuclei without triggering extensive nucleation of the randomly oriented grains. The range of optimal processing parameters may be rather narrow, especially for thick YBCO layers. This has important implications for large-scale processing of coated conductors by an *ex situ* process involving fluorinated precursors. Local variations of growth parameters caused by the nonuniformity of the gas flow pattern and temperature in a large *ex situ* reactor would result in local changes of the growth thermodynamics. These changes may either promote the nucleation of randomly oriented YBCO grains or retard the nucleation of *c*-axis oriented YBCO, thus causing granularity (growth of large grains) of the films. Both of these phenomena are equally damaging for the critical currents of the conductors. Results of this study point out the importance of uniform process conditions throughout the conductor during large-scale manufacturing of coated conductors with thick YBCO coats.

ACKNOWLEDGMENTS

The authors greatly appreciate the generosity of the American Superconductors Corporation in providing a substantial length of their metallic substrates for this study. This manuscript has been authored by Brookhaven Science Associates, LLC under Contract No. DE-AC02-98CHI-886 with the U. S. Department of Energy.

[1]Special issue, "High Performance YBCO-coated Superconducting Wires, MRS Bull. **29** (2004).
[2]S. R. Foltyn, P. Tiwar, R. C. Dye, M. Q. Le, and X. D. Wu, Appl. Phys. Lett. **63**, 1848 (1993); S. R. Foltyn, Q. X. Jia, P. N. Arendt, L. Kinder, Y. Fan, and J. F. Smith, *ibid.* **75**, 3692 (1999).
[3]S. R. Foltyn, H. Wang, L. Civale, Q. X. Jia, P. N. Arendt, B. Maiorov, Y. Li, M. P. Maley, and J. L. MacManus-Driscoll, Appl. Phys. Lett. **87**, 162505 (2005).
[4]S. Kang, A. Goyal, J. Li, A. A. Gapud, P. M. Martin, L. Heatherly, J. R. Thompson, D. K. Christen, F. A. List, M. Paranthaman, and D. F. Lee, Science **311**, 1911 (2006).
[5]B. Maiorov, H. Wang, S. R. Foltyn, Y. Li, R. DePaula, L. Stan, P. N. Arendt, and L. Civale, Supercond. Sci. Technol. **19**, 891 (2006).
[6]U. Schoop, M. W. Rupich, C. Thieme, D. T. Verebelyi, W. Zhang, X. Li, T. Kodenkandath, N. Nguyen, E. Siegal, L. Civale, T. Hlesinger, B. Maiorov, A. Goyal, and M. Paranthanman, IEEE Trans. Appl. Supercond. **15**, 2611 (2005).
[7]R. Feenstra, D. K. Christen, J. D. Budai, S. J. Pennycook, D. P. Norton, H. H. Lowndes, C. E. Klanbunde, and N. D. Galloway, *Proceedings of Symposium A-1, High Temperature Superconducting Films at the International Conference on Advanced Materials*, edited by L. Correra(Amsterdam, North Holland, 1991), p. 331.
[8]V. F. Solovyov, H. J. Wiesmann, and M. Suenaga, Physica C **353**, 14(2001).
[9]V. F. Solovyov, H. J. Wiesmann, Q. Li, D. O. Welch, and M. Suenaga, J. Appl. Phys. **99**, 013902 (2006).
[10]A. Goyal, D. P. Norton, J. D. Budai, M. Paranthaman, E. D. Specht, D. M. Kroeger, D. K. Christen, Q. He, B. Saffian, F. A. List, D. F. Lee, P. M. Martin, C. E. Klabunde, E. Hartfield, and V. L. Sikka, Appl. Phys. Lett. **69**, 1795 (1996).
[11]L. Wu, Y. Zhu, V. F. Solovyov, H. J. Wiesmann, A. R. Moodenbaugh, R. L. Sabatini, and M. Suenaga, J. Mater. Res. **16**, 2869 (2001).
[12]L. Wu, Y. Zhu, V. F. Solovyov, H. J. Wiesmann, A. R. Moodenbaugh, and M. Suenaga, Appl. Phys. Lett. **80**, 419 (2002).
[13]V. F. Solovyov, H. J. Wiesmann, L. Wu, M. Suenaga, K. Venkataraman, and V. A. Maroni, Physica C **415**, 125 (2004).
[14]V. F. Solovyov, H. J. Wiesmann, L. Wu, Y. Zhu, and M. Suenaga, IEEE Trans. Appl. Supercond. **11**, 2939 (2001).
[15]T. Siegrist, S. Sunshine, D. W. Murphy, R. J. Cava, and S. M. Zahurak, Phys. Rev. B **35**, 7137 (1987).
[16]D. M. Feldmann *et al.*, J. Mater. Res. **21**, 923 (2006).
[17]D. Dimos, P. Chaudhari, J. Mannhart, and F. K. LeGoues, Phys. Rev. Lett. **61**, 219 (1988).
[18]V. Maroni (unpublished).

Downloaded 12 Sep 2007 to 130.199.3.130. Redistribution subject to AIP license or copyright, see http://jap.aip.org/jap/copyright.jsp